NEW-TPI thermoplastic polyimide: dielectric and dynamic mechanical relaxation*

Peter Pengtao Huo and Peggy Cebe†
Department of Materials Science and Engineering, Massachusetts Institute of Technology, Cambridge, MA 02139, USA
(Received 30 April 1992; revised 23 July 1992)

The dielectric and dynamic mechanical relaxation behaviours of the thermoplastic polyimide, NEW-TPI, have been investigated from 150 to 350°C, which spans the glass transition region. Dynamic modulus at 1 Hz is about 2.2 GPa below the glass transition temperature, T_g, decreasing to 0.02 GPa in amorphous NEW-TPI, and 0.15 GPa in semicrystalline NEW-TPI, above T_g. Dielectric constant at 10 kHz is about 3.21 below T_g, increasing to 3.44 in amorphous NEW-TPI, and 3.33 in semicrystalline NEW-TPI, above T_g. Williams–Landel–Ferry (WLF) plots for amorphous and one representative semicrystalline NEW-TPI were constructed from thermal, dynamic mechanical and dielectric relaxation data but the data could not be fitted to a single master curve. Dielectric relaxation intensity, $\Delta\varepsilon = \varepsilon_s - \varepsilon_\infty$, was shown to be structure sensitive above T_g. For both semicrystalline and amorphous NEW-TPI, the relaxation intensity decreases as temperature increases. This implies that $\Delta\varepsilon$ has the same temperature dependence for the semicrystalline sample compared to the quenched amorphous polymer. This trend is different from that observed in either poly(ether ether ketone) or poly(phenylene sulphide). Our results confirm thermal analysis of NEW-TPI and show that NEW-TPI has a very small amount of tightly bound, or rigid, amorphous material, which relaxes completely within a narrow temperature range just above the T_g of the less tightly bound, or mobile, amorphous material.

(Keywords: thermoplastic polyimide; dielectric relaxation; dynamic mechanical relaxation)

INTRODUCTION

The aromatic polyimide, NEW-TPI, has been shown to be a very promising material in terms of its superior mechanical properties, high temperature stability, solvent resistance and melt processability[1–9]. Introduction of flexible units and *meta* linkages onto the polymer backbone is shown to lower the glass transition temperature, T_g, and improve processability[10]. The chemical structure has been reported previously[1], and consists of a dianhydride component, pyromellitic dianhydride (PMDA) and a diamine comprising phenyl-ether and phenyl-phenyl units:

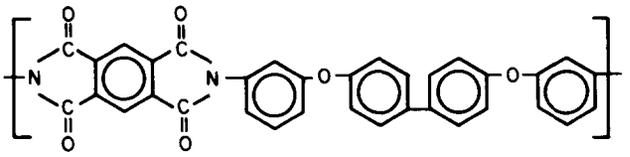

So far, very few studies have been reported on the NEW-TPI crystal lattice structure[6], morphology[7], mechanical properties subjected to irradiation[9], development of crystallinity[12], and crystallization kinetics, thermal properties and phase behaviour[11]. Our preliminary result on the dielectric study of NEW-TPI has been presented in abbreviated form elsewhere[12]. Here we report the extensive dielectric and dynamic mechanical relaxation behaviours for both amorphous and semicrystalline NEW-TPI.

We have previously utilized dielectric relaxation methods to study amorphous phase mobility in poly(ether ether ketone) (PEEK)[13], and poly(phenylene sulphide) (PPS)[14,15]. The tightly bound, or rigid, amorphous fraction exhibits decreased molecular mobility when probed calorimetrically[16–22]. The fraction of tightly bound amorphous chains (which will be referred to as 'rigid' in keeping with its prior identification[16–22]), has been deduced from heat capacity measurements using differential scanning calorimetry (d.s.c.)[16–22]. Polymers containing rigid amorphous chains were modelled according to a three-phase model comprising the crystal phase fraction, χ_c, rigid amorphous fraction, χ_{ra}, and liquid-like amorphous phase fraction, χ_a where:

$$\chi_c + \chi_{ra} + \chi_a = 1 \quad (1)$$

The idea that crystals constrain the amorphous phase has long been recognized. The morphology of semicrystalline polymers comprising lamellar crystals, amorphous material, and a intermediate region at the crystal/amorphous interphase is well known[17,23–29]. Although a large fraction of the amorphous chains may be considered to be located in the interphase (see for example, ref. 17), in many semiflexible chain polymers all the amorphous chains attain the mobility level of the liquid-like state as temperature is increased to just above T_g. However, in certain other polymers it has been shown that a portion of the amorphous phase remains rigid above T_g, conclusions which were based on observation of a negative deviation of the heat capacity increment in

* Presented at 'Advances in Polymeric Matrix Composites', 5–10 April 1992, San Francisco, CA, USA
† To whom correspondence should be addressed

0032-3861/93/040696-09

semicrystalline samples [16–22]. The location of this tightly bound amorphous material, and its relationship to the lamellar crystals, is not known but it was suggested that it may relate to strain at the crystal/amorphous interphase[21,22].

One limitation in the study of amorphous PPS and PEEK is that both cold crystallize rapidly when heated during d.s.c. above T_g[11,13,14,21,22]. The dielectric response of the quenched amorphous phase in these two polymers cannot be measured over a wide temperature range above T_g because of the rapid crystallization within 10–15°C above T_g. It is necessary to extrapolate the amorphous phase dielectric behaviour to higher temperature in order to compare with the amorphous phase in the semicrystalline polymer[13–15]. However, as shown in a separate work[11], NEW-TPI is a polymer which crystallizes very slowly compared with PPS and PEEK. The polymer remains amorphous up to a temperature nearly 50°C above T_g before crystallizing during d.s.c. scanning. Thus, NEW-TPI allows a more direct comparison of the amorphous phase dielectric behaviour in the quenched or semicrystalline polymer. Here, we utilize the broad temperature and frequency range of dielectric and dynamic mechanical relaxation to study the relaxation behaviour of NEW-TPI.

EXPERIMENTAL

NEW-TPI was synthesized by Mitsui Toatsu Chemical Co., and film processed by Foster Miller by extrusion from pellets. The as-received NEW-TPI is a transparent amorphous unoriented film as seen from absence of Bragg scattering peaks in the wide-angle diffractogram, and equality of heats of crystallization and melting in d.s.c.[4]. The as-received film was dried in a Mettler hot stage at 150°C for 20 h, then relaxed at 260°C for 20 h prior to testing[4,5]. This treatment was used to prepare all films used in this study. These treated films will hereafter be referred to either as amorphous, or according to their subsequent crystallization history. The cold crystallization temperature was 300°C, and the variable was the crystallization time, t_c. Our thermal data[11] show that as a function of t_c at 300°C we have the following weight fractions: $t_c = 10$ min: $\chi_c = 0.22$, $\chi_a = 0.64$, $\chi_{ra} = 0.14$; $t_c = 3$ h: $\chi_c = 0.27$, $\chi_a = 0.63$, $\chi_{ra} = 0.10$. Here, the crystallinity was obtained from the ratio of the heat of fusion of the semicrystalline samples to that of the perfect NEW-TPI crystal which is $\sim 139\ J\ g^{-1}$, according to data provided by Mitsui Toatsu[5]. The value of the crystallinity is very consistent with our wide-angle X-ray scattering (WAXS) data[11]. The purpose here is to make a comparison between results obtained dielectrically and those obtained by d.s.c., real time small angle X-ray scattering (SAXS) and WAXS[11].

Dynamic mechanical relaxation experiments were performed using a Seiko DMS 200 system using a heating rate of $2°C\ min^{-1}$ and measurement frequencies from 1 to 50 Hz, under nitrogen gas flow. Sample lengths were 10 mm and the cross-sectional areas were about $0.5\ mm^2$ with measurement accuracy of $0.001\ mm^2$. Amorphous sample and semicrystalline samples, cold crystallized at 300°C for 1 h, were studied using dynamic mechanical analysis (d.m.a.) over a temperature range of 200–350°C. Dielectric relaxation experiments were performed using a Hewlett Packard impedance analyser, over a temperature range of 150–320°C at frequencies from 1 kHz to 1 MHz. Both d.m.a. and dielectric experiments cover a temperature from well below T_g to nearly 100°C above T_g. Experimental details and theory of the dielectric measurement have been presented in previous work[13,14]. We define d.s.c. T_g as the mid-point of the glass transition region of d.s.c. at scan rate of $20°C\ min^{-1}$, and the dielectric T_g as the temperature of maximum $\tan\delta$ at 10 kHz. For dynamic mechanical relaxation, d.m.a. T_g can be defined as the position either of maximum $\tan\delta$ or of E''. This will be discussed in more detail below.

RESULTS AND DISCUSSION

Temperature and frequency dependent mechanical response

Dynamic mechanical relaxation results at 200–350°C are shown in *Figures 1a* and *b* for semicrystalline NEW-TPI sample cold crystallized at 300°C for 1 h. We present the dynamic modulus E' and loss factor $\tan\delta$ at frequencies of 1, 10 and 50 Hz. The modulus (*Figure 1a*) is quite flat at 2.2 GPa prior to T_g (i.e. below 255°C). Then a sharp decrease near 260°C can be observed due to the softening of the polymer at T_g, with modulus decreasing to 0.15 GPa at temperatures above T_g. This decrease takes place over a temperature range of only 40°C, from 260 to 300°C. The rubbery plateau of E' was

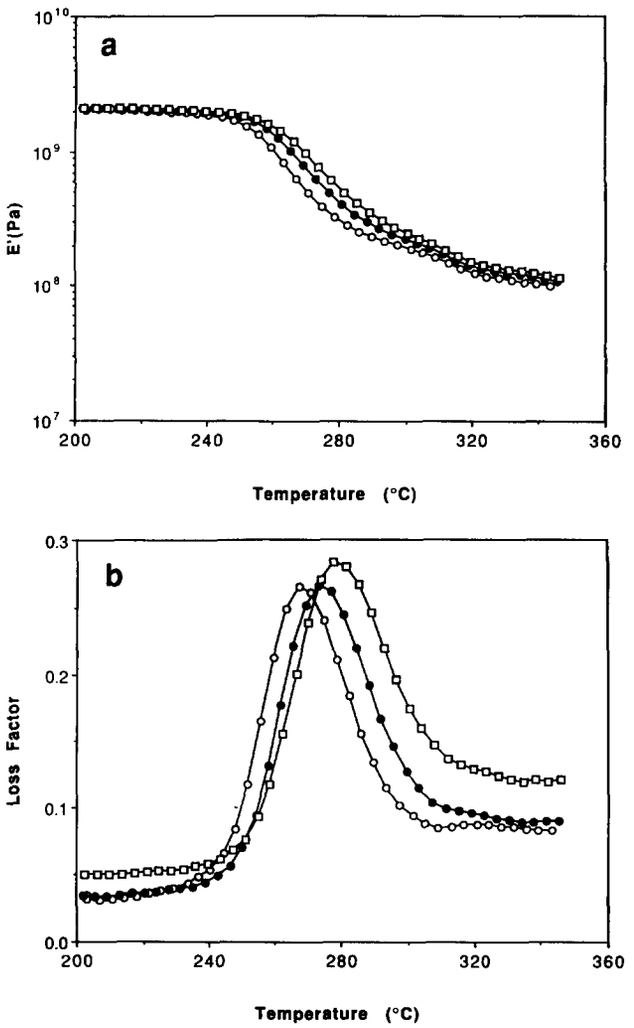

Figure 1 (a) Dynamic modulus E' and (b) loss factor ($\tan\delta$) as a function of temperature for semicrystalline NEW-TPI at various frequencies: ○, 1 Hz; ●, 10 Hz; □, 50 Hz

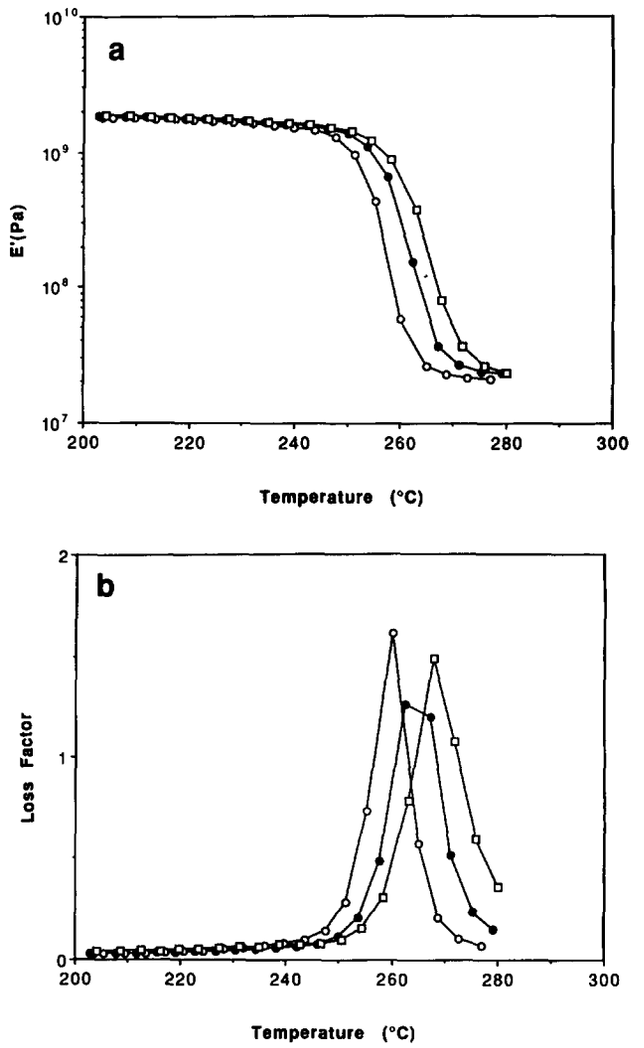

Figure 2 (a) Dynamic modulus E' and (b) loss factor ($\tan\delta$) as a function of temperature for amorphous NEW-TPI at various frequencies: ○, 1 Hz; ●, 10 Hz; □, 50 Hz

observed above 300°C. Tan δ (*Figure 1b*) has a very symmetric peak at about the same position, with a maximum from 270 to 300°C dependent on the frequency. The peak position of the tan δ shifts to higher temperature as the frequency increases. There exists a very weak relaxation process at a temperature from about 300 to 320°C, due to partial melting. The sample crystallized at 300°C has a dual endothermic response, with lower melting point at 315°C according to d.s.c. analysis[11].

For the amorphous NEW-TPI, the modulus and tan δ are shown in *Figures 2a* and *b*. The modulus of the amorphous sample (*Figure 2a*) has the usual characteristics of a glass transition, showing a decrease of almost two decades, from 2.0 GPa at 255°C to 20 MPa at 285°C, a much larger decrease than that of the semicrystalline sample. Tan δ, the position of which increases as the frequency increases, shows a much sharper and stronger peak compared with the semicrystalline sample shown in *Figure 1*. The peak full width at half maximum is only about 15°C, while it is 40°C for the semicrystalline sample. The maximum value of tan δ is about 1.5–1.7, which is about six times larger than that of the semicrystalline sample shown in *Figure 1*. This is simply because the semicrystalline NEW-TPI can be viewed as a composite of crystal and amorphous material. Only the amorphous portion can relax at T_g, and since there is a reduced amorphous phase fraction in the semicrystalline polymer, tan δ has a smaller maximum value than that of the amorphous sample.

The value of tensile modulus, E', measured at low temperature matches well with the value reported previously[5], which is 2.8 GPa at 25°C and 1.9 GPa at 150°C. To our knowledge, there has been no detailed work about the crystallinity effect on the mechanical properties, such as tensile modulus and loss factor. However, Hirade *et al.*[10] studied the effect of irradiation on the shear modulus for NEW-TPI. Their results indicate that the irradiation has significantly upshifted the T_g, while it seems to have a smaller effect on the shear modulus.

Temperature and frequency dependent dielectric response

Dielectric relaxation results in the temperature range 150–320°C are shown in *Figures 3a* and *b* for semicrystalline NEW-TPI crystallized at 300°C for 1 h. The value of ε' (*Figure 3a*) is nearly constant at 3.2 prior to the relaxation, then increases sharply at T_g. The high-temperature value of ε' was observed to decrease slightly above 300°C. The loss factor, tan δ (*Figure 3b*) shows the usual shape, reaching a maximum value of 0.01. The peak position of tan δ shifts to higher temperature and the peak maximum increases with increasing frequency.

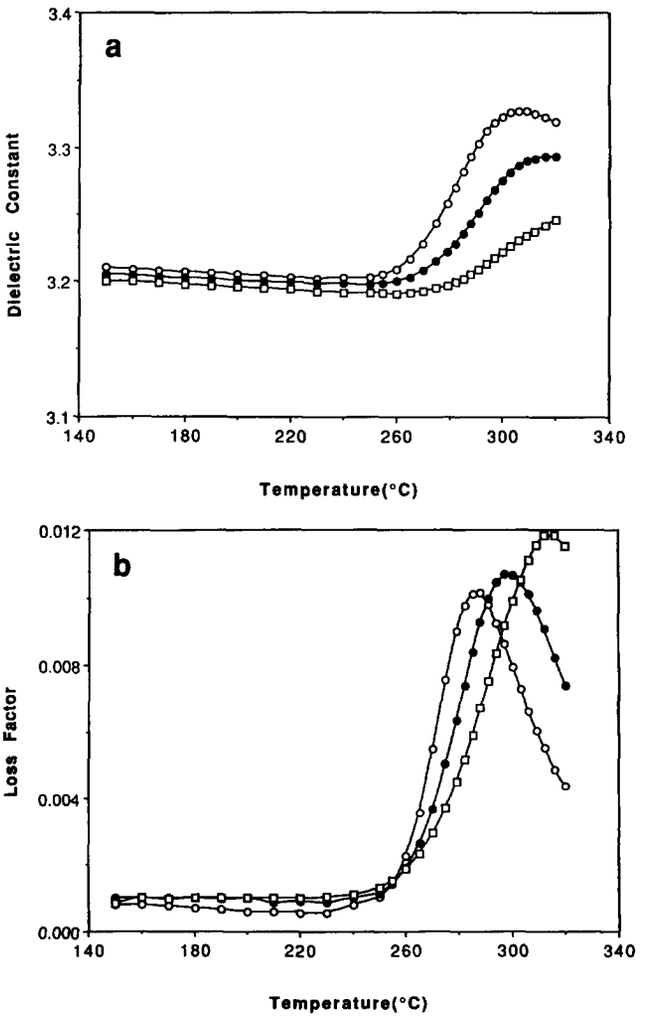

Figure 3 (a) Dielectric constant (ε') and (b) loss factor ($\tan\delta$) as a function of temperature for semicrystalline NEW-TPI at various frequencies: ○, 10 kHz; ●, 100 kHz; □, 1 MHz

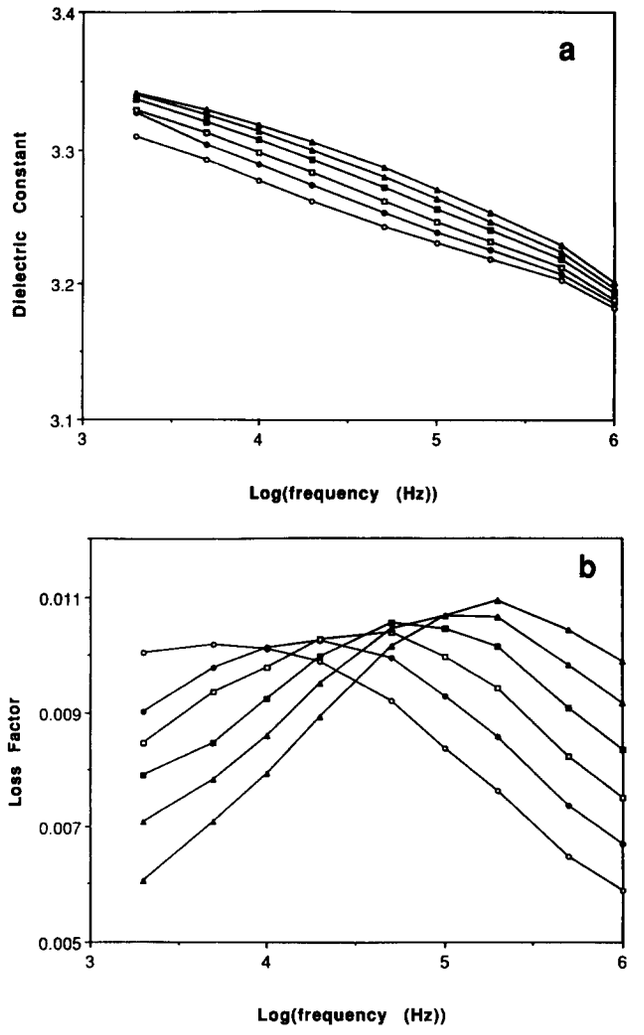

Figure 4 (a) Dielectric constant (ε') and (b) loss factor ($\tan\delta$) as a function of log(frequency) for semicrystalline NEW-TPI at various temperatures: ○, 285°C; ●, 288°C; □, 291°C; ■, 294°C; △, 297°C; ▲, 300°C

A dielectric relaxation map of the cold crystallized NEW-TPI is shown in *Figures 4a* and *b* for all the frequencies studied. ε' is shown as a function of $\log(f)$ for a series of temperatures in the vicinity of the glass transition relaxation process. In the temperature range of 270–300°C, ε' decreases as frequency increases for a fixed temperature, and at a fixed frequency, ε' decreases with decreasing temperature. The $\tan\delta$ results (*Figure 4b*) indicate a shift in the frequency of the peak maximum to higher frequency as the temperature increases.

Plots of ε' and $\tan\delta$ for amorphous film are shown in *Figures 5a* and *b* for several frequencies. At temperatures below T_g, the dielectric constant ε' is almost the same as that of the semicrystalline sample. The glass transition relaxation begins at around 250°C and ε' increases strongly to a maximum at about 300°C. The crystallization of the amorphous film above 294°C results in a slight change in the slope of ε' *versus* T, but ε' still increases a little as temperature increases.

The loss factor (*Figure 5b*) is also slightly affected by the crystallization. First, the amorphous film undergoes its glass transition relaxation and $\tan\delta$ shows a strong maximum, reaching a value of about 0.03, which shifts clearly to higher temperature with increasing frequency. $\tan\delta$ then decreases sharply as temperature increases beyond the glass transition relaxation, and the onset of crystallization occurs. A very small shoulder is seen at higher temperature in *Figure 5b* (around 310°C for 10^6 Hz). This shoulder is due to relaxation of the now-crystalline sample whose amorphous portion becomes constrained a little by the existence of crystals and therefore has a slightly higher T_g.

The relaxation maps of the amorphous NEW-TPI are shown in *Figures 6a* and *b* for all frequencies studied. The range of temperatures shown spans the glass transition region. At fixed temperature, ε' decreases with increasing frequency, as in the semicrystalline NEW-TPI. At fixed frequency ε' decreases with decreasing temperature. The loss factor (*Figure 6b*) indicates a shift in the loss peak maximum frequency to higher frequency with increasing temperature.

The dielectric constant of both amorphous and semicrystalline NEW-TPI has a value of 3.2 for 10 kHz at temperatures below T_g. This value is exactly within the range reported previously for room temperature measurement, showing ε' is 3.2 at 1 kHz and 3.1 at 1 MHz[5]. The dielectric constant of amorphous NEW-TPI at temperatures above T_g is significantly larger than that of the semicrystalline sample. The loss factor, $\tan\delta$, though basically no different at low temperature for both amorphous and semicrystalline samples, has a very

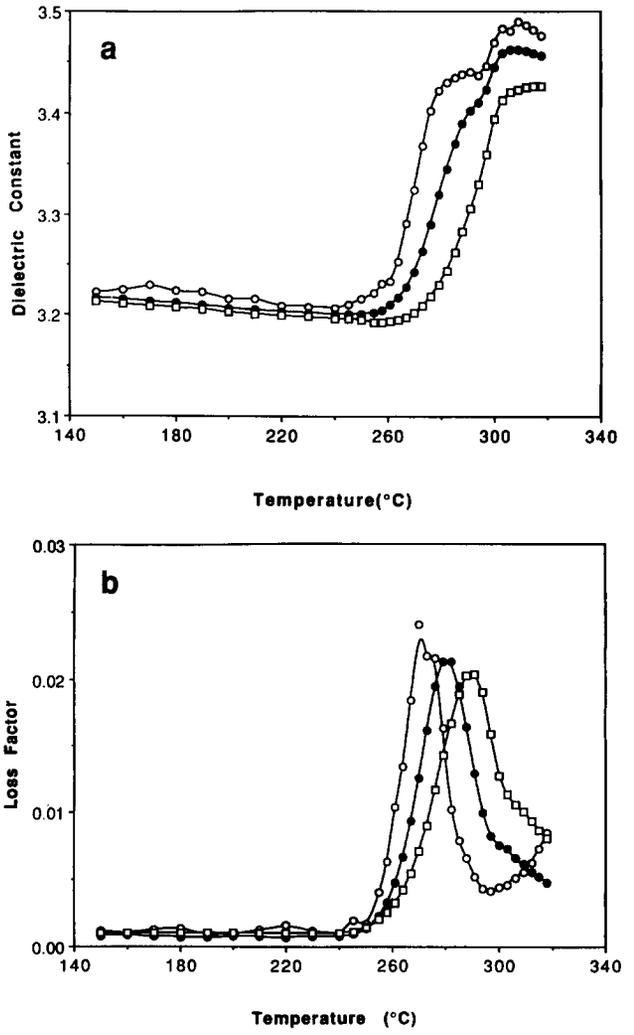

Figure 5 (a) Dielectric constant (ε') and (b) loss factor ($\tan\delta$) as a function of temperature for amorphous NEW-TPI at various frequencies: ○, 10 kHz; ●, 100 kHz; □, 1 MHz

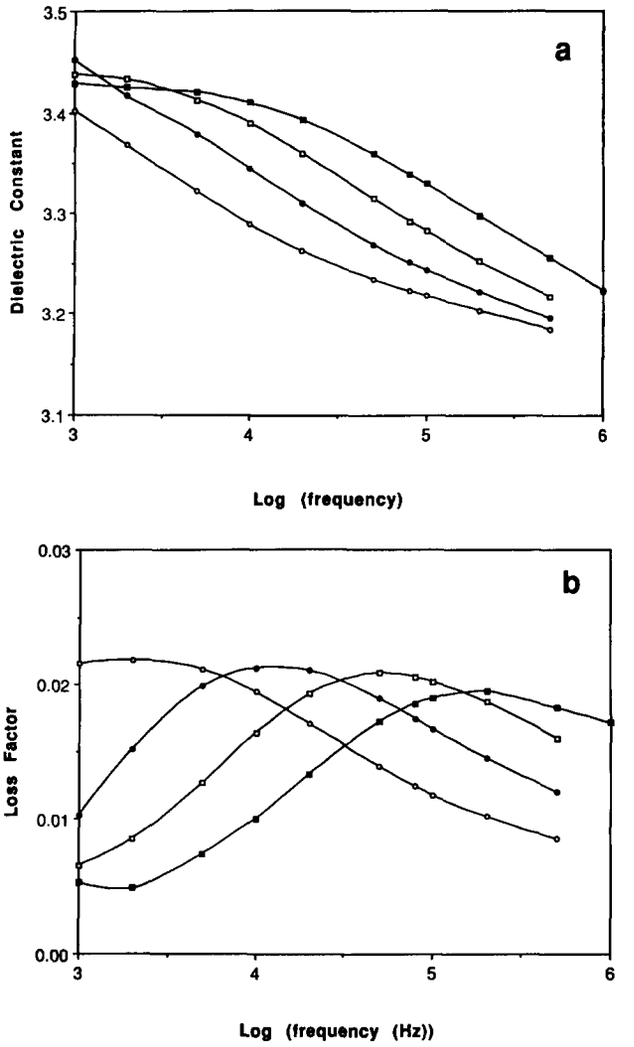

Figure 6 (a) Dielectric constant (ε') and (b) loss factor ($\tan\delta$) as a function of log(frequency) for amorphous NEW-TPI at various temperatures: ○, 276°C; ●, 282°C; □, 288°C; ■, 294°C

different value at its maximum. The amorphous sample loss factor again is twice as large as that of the semicrystalline sample.

For amorphous NEW-TPI, the effect of crystallization during heating is much smaller compared with that of PPS[14,30] and PEEK[13,31] amorphous samples. First, as shown in a separate study[11], we found relatively slow crystallization kinetics of amorphous NEW-TPI from the rubbery amorphous state[4] and a small final crystallinity (about 0.25 or less). Also, we found from d.s.c. that the T_g of amorphous NEW-TPI is about the same as for semicrystalline NEW-TPI. In the dielectric relaxation experiment here, we only observed a decrease in the increasing slope of ε' at the glass transition region, and a very small, indistinct, shoulder in $\tan\delta$ due to the slow crystallization kinetics and small ultimate crystallinity. On the other hand, for PPS and PEEK, both ε' and $\tan\delta$ are significantly affected by crystallization about 10–15°C above T_g[13,14]. We know from calorimetric studies[11] that the T_g of the amorphous NEW-TPI is only 5°C below T_g for semicrystalline NEW-TPI. From dielectric results we see that the $\tan\delta$ maximum of amorphous NEW-TPI is close to that of the now-semicrystalline sample. This explains why we see only a small shoulder for NEW-TPI instead of a distinct peak as seen for PPS and PEEK. This is because the two relaxation peaks are overlapped for NEW-TPI, while they are separated by about 20°C for PPS[14] and PEEK[13].

Temperature–frequency analysis for NEW-TPI

Dielectric relaxation and dynamic mechanical relaxation are widely used to study the glass transition behaviour of both amorphous and semicrystalline polymers. These techniques together allow the investigation of a wide range of frequency and temperature. Both techniques were combined with d.s.c. to investigate the glass transition behaviour in NEW-TPI. Usually, the maximum of the $\tan\delta$ for fixed frequency is assigned as the T_g for that particular frequency. We will refer to T_g determined from the loss factor maximum in the dynamic mechanical relaxation experiments as d.m.a. T_g.

Figures 7a and *b* show plots of log(frequency) *versus* the reciprocal temperature for semicrystalline and amorphous NEW-TPI samples, respectively. Here, the maximum positions for dielectric $\tan\delta$ and ε'' are nearly identical, and the data points completely overlap each other, so that the ε'' data cannot be separately identified. D.s.c. heating rate was transformed to an equivalent frequency according to the method reported previously[32,33]. As can be seen clearly, the dielectric T_gs, whether determined using $\tan\delta$ or ε'', are all located on the same curve, and show no constancy of activation energy for the glass transition relaxation process. Since both dielectric relaxation and dynamic mechanical relaxation deal with the glass transition process, from the temperature–frequency superposition principle, we might expect the d.m.a. T_g and dielectric T_g also to lie on the *same* curve which comprises the Williams–Landel–Ferry (WLF) plot of NEW-TPI. But from *Figure 7a* we see that whereas the dielectric $\tan\delta$ and ε'' data are coincident, this is not the case for the d.m.a. $\tan\delta$ and E'' data. Only the d.m.a. T_g data from E'' lie on the same curve as the dielectric data; the d.m.a. T_g data from $\tan\delta$ maximum are shifted towards the higher temperature side in semicrystalline NEW-TPI.

For dielectric relaxation, the position of $\tan\delta$ maxima ($\tan\delta = \varepsilon''/\varepsilon'$) and ε'' are almost the same, due to the relatively small change of ε' before and after the glass transition relaxation. In fact, the shape of the dielectrically determined $\tan\delta$ (shown in *Figure 1b*) and ε'' (which is not shown) as a function of temperature look almost identical. However, for dynamic mechanical relaxation, E' has a relatively large change before and after the glass transition, decreasing several decades after the glass transition compared with the value before the glass transition. This makes the maximum of $\tan\delta$ almost 8–9°C higher than that determined by E''. Similarly, in *Figure 7b*, the same behaviour is observed for the amorphous NEW-TPI. D.m.a. T_g defined as the $\tan\delta$ maximum is not located on the same curve as dielectric T_g. And, when E'' maximum instead of $\tan\delta$ is used as T_g for d.m.a., they are still not located on the same curve as the dielectrically determined T_g.

Thus it is seen that the definition of T_g is very critical, especially when data from different measurement techniques are compared, such as the d.m.a. and dielectric data compared here. For the same technique, consistent T_g information can be obtained no matter whether $\tan\delta$ or ε'' maximum is used. When covering a wide range of frequency and temperature by combining several techniques, there is no physical basis for choosing which

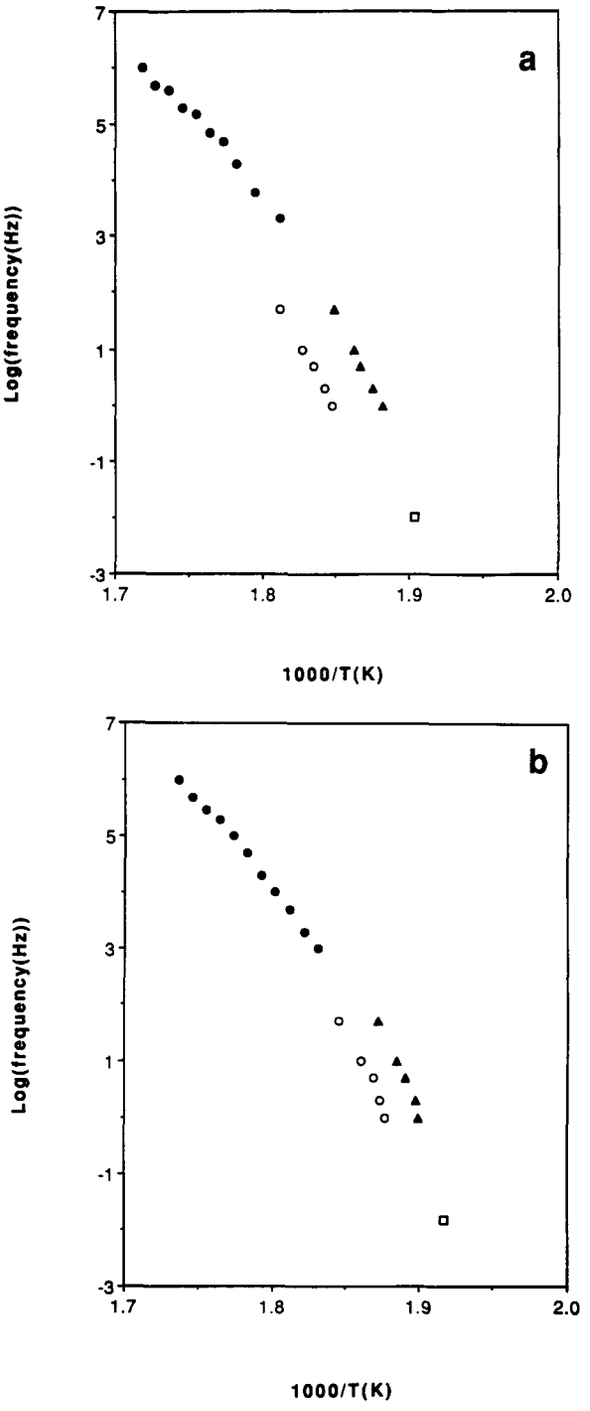

Figure 7 WLF plot for (a) NEW-TPI cold crystallized at 300°C for 1 h, and (b) amorphous NEW-TPI: ●, dielectric tan δ; ◇, ε''; ○, d.m.a. tan δ; ▲, d.m.a. E''; □, d.s.c. Data points for dielectric tan δ and ε'' completely overlap and cannot be separately identified

should be used. Due to this uncertainty, we made no attempt to fit our data to the WLF equation[26].

Dielectric relaxation intensity

The modified Debye equations have been used to describe the glass transition relaxation process for NEW-TPI as for PPS and PEEK[13,14]. The complex dielectric function, $\hat{\varepsilon}$, was modelled by Havriliak and Negami[34]:

$$\hat{\varepsilon} = \varepsilon_\infty + \frac{(\varepsilon_s - \varepsilon_\infty)}{[1 + (i\omega\tau)^{a_1}]^{a_2}} \quad (2)$$

where a_1 and a_2 are empirical parameters $(0 < a_i < 1)$ that describe the degree of departure from the Debye equations[35] (in which $a_1 = a_2 = 1$). The assumption that $a_2 = 1$ was used since we found that the Cole–Cole plots of ε'' *versus* ε' for both amorphous and semicrystalline NEW-TPI were very symmetric. We therefore chose to fit our data using the minimum number of adjustable parameters, by fitting to a circle with origin displaced below the $\varepsilon'' = 0$ line[36].

A non-linear least squares fitting routine[37] was used to find a_1, ε_s and ε_∞, which were the only adjustable parameters[13–15]. Examples of Cole–Cole plots are shown in *Figures 8a* and *b*, for the semicrystalline and amorphous dielectric relaxations, respectively. Symbols represent the data points; however, not all the points were used in the fitting. For example, in *Figure 8a* the highest frequency data point represents the onset of a second process, and was not used to fit the glass transition relaxation. From the circle intersection with the ε' axis, we see the temperature dependence of the difference between the upper intersection (ε_s) and lower one (ε_∞). This is the dielectric relaxation intensity ($\Delta\varepsilon$)[35], which is defined as:

$$\Delta\varepsilon = \varepsilon_s(T) - \varepsilon_\infty(T) \quad (3)$$

where subscripts s and ∞ refer respectively to static (low) frequency and infinite (high) frequency of measurement relative to the process under study.

The dielectric relaxation intensity, $\Delta\varepsilon(T)$ *versus* temperature is shown in *Figure 9* for amorphous NEW-TPI and NEW-TPI cold crystallized at 300°C for 10 min and 3 h. The straight line is the best fit to the measured data. The dielectric relaxation intensity is greater, the shorter the cold crystallization time of the NEW-TPI. This can be readily interpreted by considering the crystallization time dependence of the degree of crystallinity from our thermal analysis study[4,11]. The semicrystalline NEW-TPI has a smaller degree of crystallinity when cold crystallized at 300°C for shorter time (see Experimental). Thus, there is a larger fraction of amorphous dipoles at short crystallization time and the intensity of the amorphous relaxation is increased. The temperature dependence of $\Delta\varepsilon$ is almost the same for amorphous and semicrystalline NEW-TPI. For amorphous NEW-TPI, the relaxation intensity shows the usual case, decreasing as temperature increases. For the semicrystalline samples, the relaxation intensity also decreases with increasing measurement temperature.

The temperature dependence of $\Delta\varepsilon$ for the amorphous sample above T_g has long been recognized, showing a decrease as a consequence of temperature increase. This trend in $\Delta\varepsilon$ has also been observed for other polymers such as PPS[14], PEEK[13] and poly(ethylene terephthalate)[38,39]. The main point here is that competition exists between thermal energy and electric field effects for dipole alignment. Increasing the thermal energy of dipoles will tend to randomize the alignment of the dipoles and therefore decrease the dielectric relaxation intensity. For semicrystalline samples, we assume that only the amorphous phase fraction can relax at temperatures above T_g, while the crystal phase is still rigid. This is what is observed in *Figure 9*, with $\Delta\varepsilon$ showing a *decrease* as temperature increases for both the quenched amorphous and semicrystalline samples. This implies that the amorphous phase inside the now-semicrystalline polymer is relaxing with about the same temperature dependence as the quenched 100% amorphous sample.

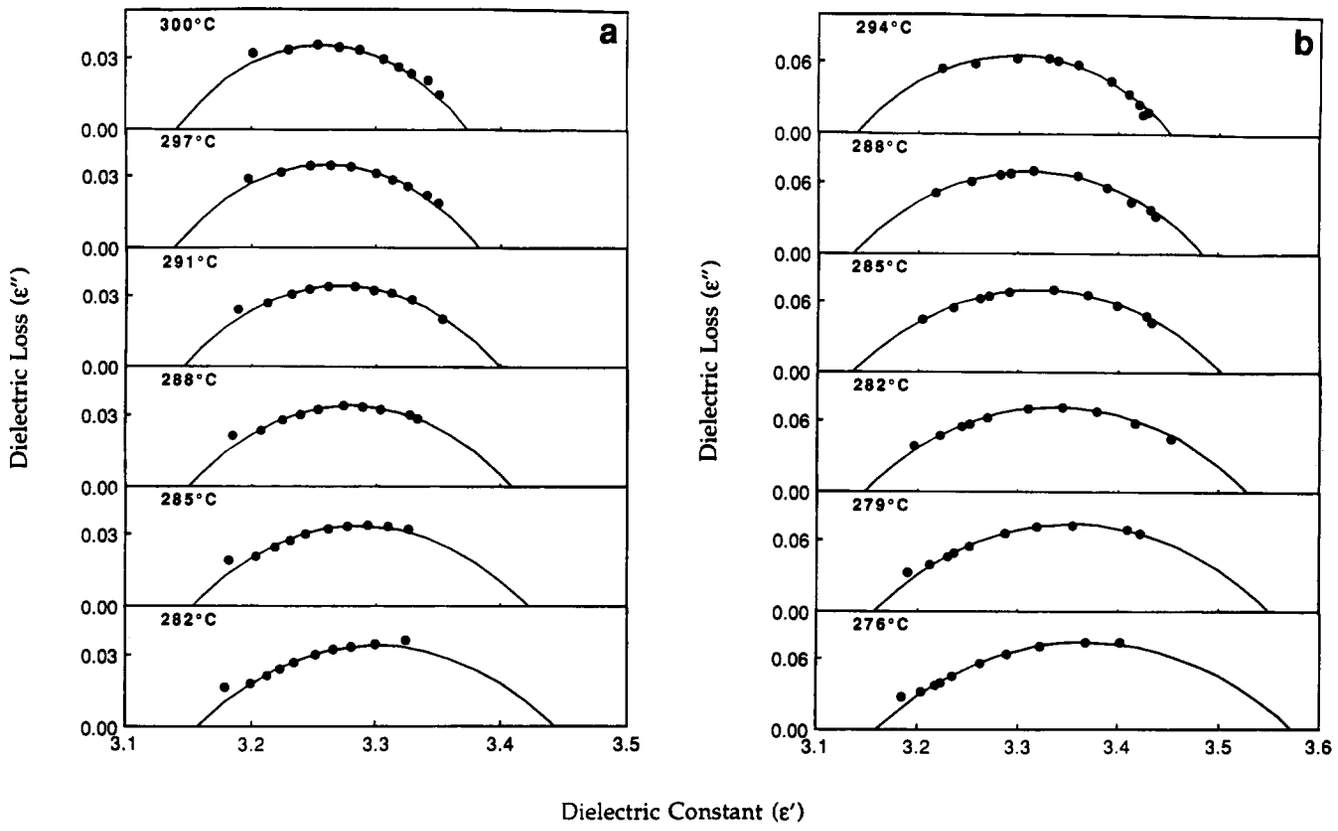

Figure 8 Cole–Cole plots for (a) NEW-TPI cold crystallized at 300°C for 1 h and (b) amorphous NEW-TPI

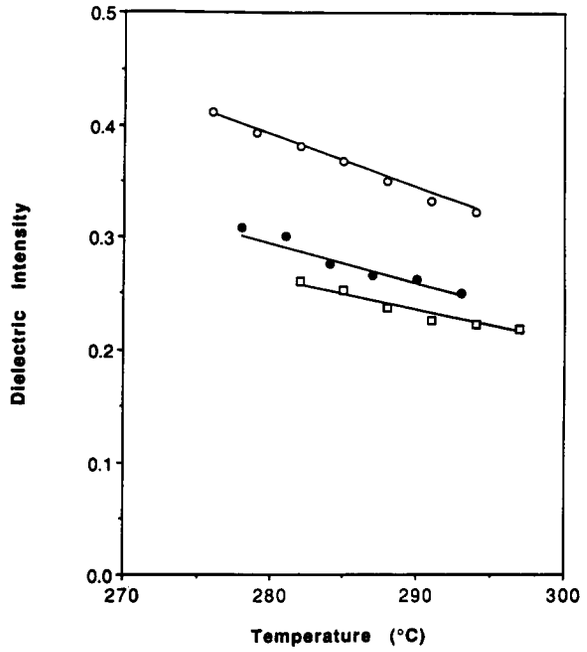

Figure 9 The dielectric relaxation intensity ($\Delta\varepsilon$) *versus* temperature for amorphous (○) and NEW-TPI cold crystallized at 300°C for 10 min (●) and 3 h (□)

The temperature dependence of relaxation strength for NEW-TPI seen in *Figure 9* is not the same as that observed in either PPS or PEEK[13–15]. In those polymers, the amorphous phase relaxation in the semicrystalline sample had a completely different temperature dependence compared to the quenched amorphous samples, leading to an *increase* in relaxation strength as temperature increased above T_g. This was explained by the existence of a large amount of tightly bound, or rigid, amorphous material in PPS and PEEK which relaxes gradually above the T_g of the mobile amorphous fraction[13,14]. In contrast to PPS and PEEK, there is only about 0.10–0.14 weight fraction of rigid amorphous material in the cold crystallized NEW-TPI. A fairly loose connection exists between the crystals and the amorphous phase in semicrystalline NEW-TPI, leading to a small amount of tightly bound amorphous material (as deduced from heat capacity measurements[11]). This small amount of rigid amorphous material relaxes within a narrow range of temperatures just above T_g. Once all the amorphous phase dipoles (liquid-like and rigid amorphous) have been relaxed, their temperature dependent relaxation strength will decrease with increasing temperature from the competition between thermal energy and electric field alignment.

In analogy to heat capacity increment, we use $\beta(T)$ as defined previously[13,14] to stand for the total fraction of dipoles relaxed at temperature T, where:

$$\beta(T)=\frac{\Delta\varepsilon(T)^{sc}}{\Delta\varepsilon(T)^{a}} \tag{4}$$

$\beta(T)$ is the temperature dependent relaxation strength of the amorphous phase in the semicrystalline sample, normalized to the strength of the amorphous phase in the 100% amorphous sample. Using equation (3), $\beta(T)$ can be written as:

$$\beta(T)=\frac{\varepsilon_s(T)^{sc}-\varepsilon_\infty(T)^{sc}}{\varepsilon_s(T)^{a}-\varepsilon_\infty(T)^{a}} \tag{5}$$

Here, the definition of $\beta(T)$ is valid at temperatures $T > T_g$. For temperature $T < T_g$, $\beta(T)=0$. Certainly, $\beta(T)$,

defined in equation (5), includes all the liquid-like amorphous phase, χ_a, obtained by the heat capacity increment and possibly some portion of tightly bound amorphous phase that is relaxed at $T > T_g$ but is considered rigid at the d.s.c. T_g. The dielectric method[13–15] has a distinct advantage over the use of heat capacity[16–22] to determine the fraction of relaxing units. First, $\beta(T)$ can be used to quantify the total amount of material that relaxes at high temperature ($T > T_g$) and does not require any prior measurement of the degree of crystallinity. Extrapolation of $\beta(T)$ to T_g of the semicrystalline sample gives χ_a, the amount of liquid-like amorphous phase, while extrapolation of $\beta(T)$ to T_m derives the total amount of amorphous material (liquid-like amorphous phase plus rigid amorphous, $\chi_a + \chi_{ra}$)[13–15]. By comparison, to determine χ_{ra} by d.s.c. heat capacity method and equation (1), we need to have the crystallinity value available, obtained either from d.s.c. heat of fusion or WAXS. Second, the temperature dependence of the relaxation above T_g is easily obtained from $\beta(T)$ *versus* T. However, it is comparatively difficult from d.s.c. analyses to obtain the change in heat capacity at temperatures higher than T_g (i.e. at temperatures above the increment in heat capacity, $C_p(T)$ at T_g) due to the relatively small absolute change in heat capacity, and to the problem of baseline determination.

In our previous works on PPS and PEEK, because of the experimental incapability of obtaining the $\Delta\varepsilon$ of the respective amorphous samples at high temperature (due to the rapid crystallization above T_g), it was necessary to extrapolate $\Delta\varepsilon$ of the amorphous polymer to high temperature. Here, for NEW-TPI, we are able to measure the $\Delta\varepsilon$ directly at temperatures even 40°C higher than T_g of the amorphous sample, because of the very slow crystallization process[4,11]. There is a significant overlap in terms of the temperature range for both amorphous and semicrystalline dielectric relaxation intensities, as can be seen in *Figure 9*. Moreover, the very slight increase of T_g of the semicrystalline sample over the amorphous sample[11] also benefits this overlap, since we can fit the Cole–Cole plot in the vicinity of the glass transition with confidence only over a certain temperature range.

The estimate of the numerical value of $\beta(T)$ for NEW-TPI semicrystalline samples allows a quantitative understanding of the relaxation and the temperature dependent mobility of the amorphous phase in NEW-TPI. Based on the amorphous phase intensity shown in *Figure 9*, our value of $\beta(T)$ calculated from equation (5) is *constant* from 278 to 300°C for each semicrystalline sample. For samples cold crystallized at 300°C either for 10 min or for 3 h, the values of $\beta(T)$ are 0.76 and 0.72, respectively. The corresponding liquid-like amorphous phase fractions determined thermally are 0.64 and 0.63 (see Experimental), and the total amorphous phase fractions ($\chi_c + \chi_{ra}$) for the same two crystallization conditions are 0.78 and 0.73. The $\beta(T)$ values thus correspond very nearly to the total amorphous phase fractions of the semicrystalline samples. Therefore, since $\beta(T)$ represents the fraction of dipoles already relaxed at temperature T, we conclude that the entire amorphous phase in NEW-TPI has become relaxed by about 278°C. The most tightly bound amorphous material (which only constitutes a small amount of the total amorphous material in NEW-TPI semicrystalline samples) becomes mobile at, or before, about 278°C, i.e. within 20°C above calorimetric T_g. Above 278°C there is no additional contribution to the relaxation and $\beta(T)$ is constant. Therefore we expect $\beta(T)$ to be equal to the total amorphous phase fraction from 278°C up to the melting temperature.

Our NEW-TPI cold crystallization study[11] shows that when NEW-TPI is isothermally cold crystallized, the kinetics can be described nearly by a single Avrami exponent over the entire crystallization period. This indicates that there is one process governing crystallization (the 'primary' process) and this persists until crystallization is complete. We suggest that the small amount of rigid amorphous material, and its ability to relax immediately as temperature increases above T_g, is related to the same factors that contribute to lack of strong secondary crystallization process in NEW-TPI. On the other hand, for PEEK polymer a large fraction of crystals develops by secondary crystallization processes[40]. Also, subsidiary lamellar crystals have been observed using transmission electron microscopy and found to be in-filling, that is, fitting in between the dominant lamellae[41], though the relationship between the bulk kinetic crystallization process and formation of subsidiary crystals is still unclear. In PEEK, these subsidiary crystals may serve to interrupt and hence constrain the amorphous phase, creating a large fraction of tightly bound, or rigid, amorphous material. As suggested before[21] the rigid amorphous fraction may be related to strain at the crystal/amorphous interface. This idea is supported by the fact that large amounts of rigid amorphous material are created under conditions of rapid cooling[14,21,42] or crystal growth from a state of low chain mobility, both of which would favour formation of a large population of small, imperfect crystals.

It is possible that imperfect, tiny secondary crystals provide a base for the rigid amorphous fraction. Indeed, for PPS and PEEK, χ_{ra} can be as large as 0.45 for PPS[14,15] and 0.35 for PEEK[13] cold crystallized samples. Here, by using dielectric relaxation experiments, we confirm the existence of a small amount of rigid amorphous material in NEW-TPI cold crystallized samples, and also provide information about the temperature dependence of the relaxation of the amorphous phase. As shown in *Figure 9*, the rigid amorphous material relaxes immediately within 20°C above T_g. This is also very different from PPS and PEEK, both of which show a gradual relaxation starting just above T_g and continuing up to the melting point of the least perfect crystals. In terms of the crystal/amorphous connection or coupling, the T_g is considered to be a good indicator. NEW-TPI semicrystalline samples which may have loosely connected crystal/amorphous regions show very small increase in T_g upon crystallization, compared with purely amorphous samples, measured both calorimetrically and dielectrically. This is also in sharp contrast to PPS and PEEK semicrystalline samples, both of which have T_gs about 20°C higher than that of purely amorphous samples.

CONCLUSIONS

Dielectric and dynamic mechanical relaxation experiments have been performed to characterize the glass transition relaxation and to explore the amorphous phase behaviour of NEW-TPI. The dielectric constant and loss factor, modulus and mechanical loss factor were measured

through the glass transition region. The dielectric relaxation intensity is structure sensitive above T_g, showing variations in magnitude with crystal and amorphous phase composition in the semicrystalline samples. With regard to the temperature dependence of the dielectric relaxation intensity, we find that $\Delta\varepsilon$ has the same temperature dependence for the semicrystalline sample compared to the quenched amorphous polymer. Our results confirm thermal analysis of NEW-TPI[11] and show that NEW-TPI has a very small amount of tightly bound, or rigid, amorphous material, which relaxes completely within a narrow temperature range just above the T_g of the less tightly bound, or mobile, amorphous material.

ACKNOWLEDGEMENT

This research was supported in part by the Petroleum Research Fund, administered by the American Chemical Society, and by the AT&T New Research Award Fund.

REFERENCES

1 Hergenrother, P. M. SPE Conference on High Temperature Polymers and Their Uses, Case Western Reserve University, 2–4 October 1989
2 Hou, T. H. and Reddy, R. M. *SAMPE Q.* 1991, January, 38
3 Friler, J. B. and Cebe, P. *Mater. Res. Soc. Symp. Proc.* 1991, **217**, 101
4 Friler, J. B. and Cebe, P. *Polym. Eng. Sci.* in press
5 Mitsui-Toatsu Chem., Inc. Tokyo, Japan. *Technical Data Sheet/A-00*
6 Sakaitani, H., Okuyama, K. and Arikawa, H. *Polym. Prepr. Jpn* 1991, **40**(1–4), 478
7 Yuasa, S., Truji, M. and Takahashi, T. *Polym. Prepr. Jpn* 1991, **40**(1–4), 491
8 Sasuga, T. *Polymer* 1991, **32**, 1539
9 Hergenrother, P. M., Wakelyn, N. T. and Havens, S. J. *J. Polym. Sci., Polym. Chem. Edn.* 1987, **25**, 1093
10 Hirade, T., Hama, Y., Sasuga, T. and Seguchi, T. *Polymer* 1991, **32**, 2499
11 Huo, P., Friler, J. B. and Cebe, P. *Polymer* in press
12 Huo, P., Friler, J. B. and Cebe, P. *Mater. Res. Soc. Symp.* 1991, **227**, 239
13 Huo, P. and Cebe, P. *Macromolecules* 1992, **25**, 902
14 Huo, P. and Cebe, P. *J. Polym. Sci., Polym. Phys. Edn* 1992, **30**, 239
15 Huo, P. and Cebe, P. *Mater. Res. Soc. Symp. Proc.* 1991, **215**, 93
16 Suzuki, H., Grebowicz, J. and Wunderlich, B. *Makromol. Chem.* 1985, **186**, 1109
17 Loufakis, K. and Wunderlich, B. *Macromolecules* 1987, **20**, 2474
18 Gaur, U. and Wunderlich, B. *J. Phys. Chem. Ref. Data* 1981, **10**, 119
19 Grebowicz, J., Lau, S. F. and Wunderlich, B. *J. Polym. Sci., Polym. Symp.* 1984, **71**, 19
20 Suzuki, H., Grebowicz, J. and Wunderlich, B. *Macromol. Chem.* 1985, **186**, 1109
21 Cheng, S. Z. D., Wu, Z. Q. and Wunderlich, B. *Macromolecules* 1987, **20**, 2802
22 Cheng, S. Z. D., Cao, M. Y. and Wunderlich, B. *Macromolecules* 1986, **19**, 1868
23 Flory, P. J. *J. Am. Chem. Soc.* 1962, **84**, 2857
24 Popli, R. and Mandelkern, R. *Polym. Bull.* 1983, **9**, 260
25 Flory, P. J., Yoon, D. Y. and Dill, K. A. *Macromolecules* 1984, **17**, 862
26 Yoon, D. Y. and Flory, P. J. *Macromolecules* 1984, **17**, 868
27 Popli, R., Glotin, M., Mandelkern, R. and Benson, R. S. *J. Polym. Sci.* 1984, **22**, 407
28 Hahn, B., Wendorff, J. and Yoon, D. J. *Macromolecules* 1985, **18**, 718
29 Hahn, B., Hermann-Schonherr, O. and Wendorff, J. H. *Polymer* 1987, **28**, 201
30 Chung, J. S. and Cebe, P. *J. Polym. Sci., Polym. Phys. Edn* 1992, **30**, 163
31 Cebe, P. *J. Mater. Sci.* 1988, **23**, 3721
32 Donth, E. *J. Non-Cryst. Sol.* 1982, **53**, 325
33 Schick, C. and Nedbal, J. *Progr. Colloid Polym. Sci.* 1988, **78**, 9
34 Havriliak, S. and Negami, S. *Polymer* 1967, **8**, 161
35 McCrum, N. G., Read, B. E. and Williams, G. 'Anelastic and Dielectric Effects in Polymeric Solids', John Wiley and Sons, New York, 1967
36 Cole, R. H. and Cole, K. S. *J. Chem. Phys.* 1941, **9**, 341
37 Bevington, P. R. 'Data Reduction and Error Analysis for the Physical Science', McGraw Hill, New York, 1969
38 Schlosser, E. and Schonhals, A. *Colloid Polym. Sci.* 1989, **267**, 963
39 Coburn, J. C. and Boyd, R. H. *Macromolecules* 1986, **19**, 2238
40 Cebe, P. and Hong, S.-D. *Polymer* 1986, **27**, 1183
41 Bassett, D. C., Olley, R. H. and Al Raheil, I. A. M. *Polymer* 1988, **29**, 1745
42 Huo, P. and Cebe, P. *Colloid Polym. Sci.* 1992, **270**, 840